# Fade-tolerant Beam Acquisition and Tracking for Optical Inter-HAP Crosslinks[1]

T. Dreischer, A. Märki, B. Thieme
Contraves Space AG
Schaffhauser Str. 580
8052 Zurich, Switzerland
+41 1 306 2024
thomas.dreischer@unaxis.com

*Abstract*—This paper reports on an enhanced method to acquire and steer an optical beam that is transmitted between two high altitude platforms in stratosphere. Overall design aspects are discussed, including considerations on atmospheric turbulence that contributes considerable fade statistics. The paper focuses on optical beam steering aspects and outlines the approach to a robust beam steering unit for optical crosslinks between HAPs, based on state-of-the-art technology. Simulation results are discussed briefly.

**TABLE OF CONTENTS**



## 1. INTRODUCTION

The reported task is part of the CAPANINA project, an EU activity under FP6. CAPANINA develops broadband capability from aerial platforms including High Altitude Platforms (HAPs) to deliver cost effective solutions providing a viable alternative to cable and satellite, with the potential to reach rural, urban and travelling users. Examples of HAPs include airships and solar powered aeroplanes operating at altitudes of around 20km, well above any air traffic. The technology developed will deliver data rates to a fixed or moving user of up to 120Mbit/s anywhere within a HAPs' 60km diameter coverage area.

In that context, optical links are expected to considerably enhance backhaul and interplatform communications. One major constraint of HAP systems is related to the aggregation of traffic.

Free-space Optical (FSO) communication systems will allow data rates of about 622Mbit/s per backhaul link in excess of that available using mm-wave bands based links. On backhaul links this capacity can be used to augment, but not replace, the mm-wave band to deliver non-time critical traffic (e.g. content distribution) in clear air conditions. The mm-wave bands are reserved for time critical traffic.

Stratospheric optical interplatform links will not suffer outages due to rain or clouds as they will be used well above cloud height at 17 km to 22 km altitude, compared with cloud heights of <13km. Next to background radiation impacts, a critical aspect of optical links is the ability of them to cope with the HAP station-keeping characteristics, including HAP rotation and vibration. The potential of the high data rates for optical HAP-HAP crosslinks is strongly related to a reliable optical beam steering and tracking under the presence of the expected HAP environmental conditions.

Contraves Space is focusing on the development of a reliable optical beam steering and tracking for optical inter-HAP crosslinks. This involves both, a simulation phase on pointing, acquisition and tracking, the overall design as well as a proof-of-concept hardware validation on breadboard level that verifies the critical items involved. Latter comprise the impact of HAP attitude motion and microvibration disturbances. The proof-of-concept hardware includes software modelling as well as the integration of complementary hardware items that have been realised in the frame of ESA projects on optical intersatellite link terminal developments (SROIL, ISLFE programme [RD 5]).

A system simulation was required for the optical crosslink analysis, to investigate the potential of state-of-the-art technologies, aiming at a feasibility statement about beam steering requirements. The simulation concept and corresponding conclusions are briefly discussed in the following sections of this paper.

[1] IST Summit '05 paper #236, version 1, April 15, 2005

## 2. SIMULATION CONCEPT

Optical transmission in the stratospheric channel has not been explored and measured, yet. Therefore, models have been built that simulate temporal fading of optical beams, including a stratospheric channel model that has been derived from measurements by the HRDI instrument on UARS [RD 1] and models derived from atmospheric measurements on the Canary islands [RD 11]. Additionally, a micro-vibration model was established similar to the well-known approach for statellites, but based on measurement data from a Zeppelin airship, as no information was yet available on vibration levels of stratospheric blimps.

All models have been integrated, together with optical interface information based on literature [RD 3, RD 4 ], into a system simulation that describes an optical crosslink between two blimps in stratosphere. The system simulation architecture bases on hardware experience at Contraves Space in the development of prototype optical terminals for intersatellite crosslinks in space [RD 6]. The system simulation model under Matlab/Simulink was adapted for stratospheric crosslinks on airship platforms.

The aim is to keep tracking a laser beam on a high-altitude platform (HAP) even if time-limited fades occur due to atmospheric inhomogeneity or due to platform vibrations of the HAP itself. Channel propagation properties have been applied to simulate an airship floating on an altitude of about 17km (worst case altitude w.r.t. turbulence).

For transmission of information over several hundred kilometers distance in the atmosphere, there are two main problems concerning acquisition and tracking the optical beam that are:

- Mechanical disturbances such as vibrations induced by the host platform.
- HAP attitude determination during (initial) acquisition.
- Atmospheric disturbances such as impurities in the air or inhomogeneity of the air density.

The general idea how to enhance the robustness of optical beam steering has been to attach inertia sensors that provide an estimation of angular displacement during a fade of the received beam. The idea of fade tolerant tracking has generally been described in [RD 8], using an analytical model for Gaussian distributed random vibration disturbances.

The analytic model for a single tracking subsystem from [RD 8] was extended for the simulation by transformation to time domain and by adding a full model of an optical inter-HAP crosslink, comprising the optical transmission channel and two fully equipped beam steering units, each attached to an independently vibrating platform. A boundary condition has been to model only components that are available today, in order to obtain by analysis a feasibility statement that is based on state-of-the-art assumptions.

## 3. SIMULATION ARCHITECTURE

As shown in Figure 1, the system simulation comprises two independent optical terminals that are linked via two independent stratospheric channel models. Each optical terminal consists of a beam steering unit (BSU), optical antennas and a microvibration generator. The stratospheric channel blocks model temporal fades, space loss and path delay, depending on link distance and wind speed.

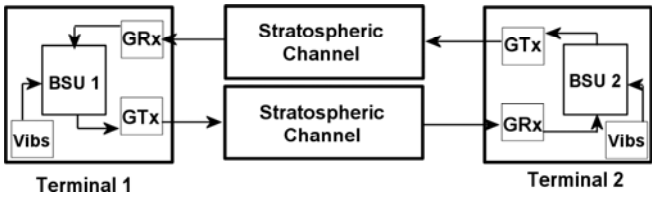


**Figure 1**–Principle block diagram of simulation architecture

### *3.1 Environmental Aspects*

*Link Distances*—The link distance for an optical HAP-HAP cross link is specified in the range between 20 km and 700 km. The lower boundary represents a first cut estimate for a minimum required HAP distance for which a HAP crosslink network becomes superior to- or as attractive as the installation of a ground based fibre network. The maximum boundary on link distances is related to maximum line-of-sight at the given minimum altitude range, with an additional constraint to stay above a maximum measured Cirrus cloud level of 13 km, as shown below in Figure 1.

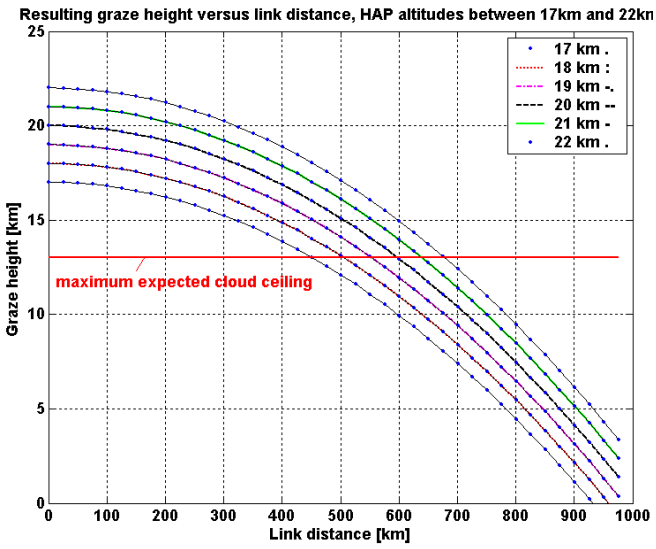


**Figure 2** – Graze height versus crosslink distance for different HAP altitudes

*Atmospheric Effects*—In a first approximation, the effect of stratospheric attenuation shall be included as a fixed value of – 2dB. Most important, however, are statistical fades that occur on the optical crosslink, as both, the receiving and the transmitting BSU are located in turbulent medium.

*Fade Depth Statistics*—Parametric simulations were made to characterise optical propagation through the stratosphere. Although being located high above the atmosphere, the influence of refractive turbulence in stratosphere is still strong enough to introduce considerable damping in the optical communication links. The reason is mainly given by the relatively high value of the structure constant of the index of refraction for heights between 10 and 17 kilometers.

Next to applied model constants and parameters, the amount of stratospheric attenuation depends also on the receive and transmit antenna diameters, wavelength and the link distance. Temporal statistics depend on windspeed. According to the available data from the University of Michigan [RD 1, RD 2] at the envisaged altitudes, the wind ranges between 30 and 40 m/s. Taking into account different angles between the wind vector and the link direction, two velocities were finally considered: 5 m/s and 40 m/s.

The simulated mean duration of fades varies from some milliseconds for windspeed equal to 5 m/s and some tenths of milliseconds for windspeed equal to 40 m/s. Fade probabilites were modelled up to minimum 10^-8. Some boundaries are given below in Table 3 for an optical crosslink between two terminals with 35mm Tx diameter and a Rx diameter of 135mm, using 1550nm wavelength.

**Table 1.** Example of attenuation characteristics for 35mm Tx/135mm Rx aperture diameter, 1550nm wavelength

| | **Probability of fade** | | | |
|---|---|---|---|---|
| **Link Distance** | **10^-1** | **10^-2** | **10^-4** | **10^-6** |
| **50 km** | 3 dB | 4 dB | 7 dB | 12 dB |
| **100 km** | 4 dB | 7 dB | 16 dB | 25 dB |
| **200 km** | 5 dB | 15 dB | 30 dB | 40 dB |
| **400 km** | 10 dB | 20 dB | 37 dB | 50 dB |

*Optical Background Levels*—Reception at daytime conditions have to cope with high background contribution by daylit sky (Table 2). This scenario is considered a worst case, additionally including partially reflected sun light from a counter station's cover. As an example for a 65m class blimp, assuming a cross section area of 1106m^2, the following flux would be received from diffuse reflected sunlight in 1 nm optical bandwidth (Table 1):

**Table 2.** Received background flux from diffuse reflected sunlight in 1nm optical filter BW, radiometric approach

| Link Distance | Center wavelength | | |
|---|---|---|---|
| | 810nm | 1064 nm | 1550 nm |
| 20km | 31.6 nW | 17.4 nW | 6.3 nW |
| 700 km | 25.8 pW | 14.2 pW | 5.1 pW |

**Table 3.** Clear Blue Sky spectral radiance (sea level , view angle 45 deg, [RD 3])

| W / cm2 / sr / µm | Center wavelength | | |
|---|---|---|---|
| | 800 nm | 1064 nm | 1550 nm |
| | 22 E-4 | 5 E-4 | 3 E-4 |

*Platform Vibration modelling*—The microvibration spectrum will be considered as a continuos random disturbance that is superimposed by transient vibration disturbances. By similarity, microvibration measurements have been taken from Zeppelin airships, as shown in Figure 3.

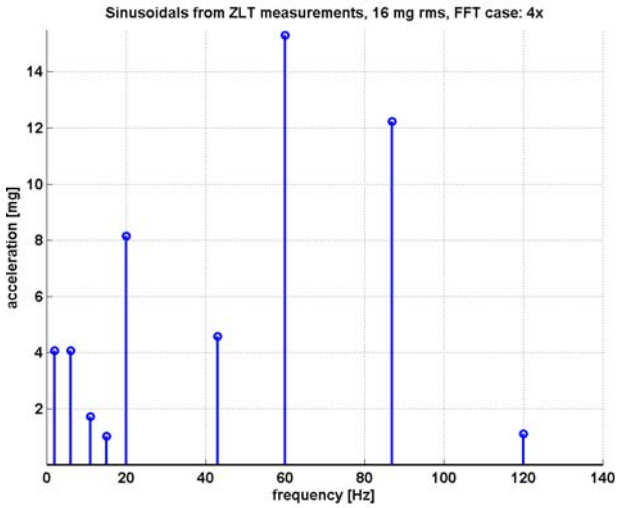


**Figure 3** – Sample Fourier spectra from Zeppelin platform

The static sinusoidals given in Figure 3 represent a typical selection from various test cases that depend on variations of motor loads, propeller speed and operation. In the numerical simulation, a validated transfer function of an optical head hardware from an ESA project was selected to transform acceleration input into rotational output about line-of-sight.

### *3.2. Optical Beam Steering Unit Architecture*

The main tasks of the Optical Beam Steering Unit comprise channel separation, beam steering and tracking. This is achieved by the interplay of an optical sub system including the telescope with coarse- and fine steering mechanisms via sensor feedbacks in a nested control loop. The simulated optical BSU comprises all subsystems and components as well as the nested controller.

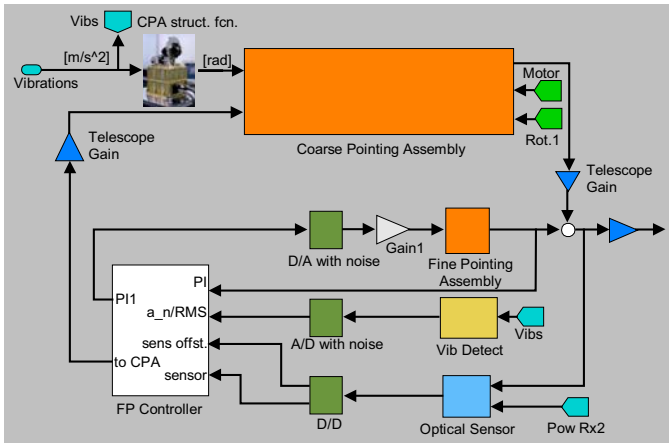


**Figure 4** – Simulation architecture of an Optical Beam Steering Unit

### *3.3. Inertia Sensing Support*

The strong fades introduced by stratospheric turbulence require special means to cope with interrupted optical feedback signals from a counter station. A cost efficient approach is to apply additional controller feedback from pairs of accelerometers, as analytically described in [RD 8]. To measure two orthogonal directions of rotation, a minimum of three accelerometers is required. Double integration of the accelerometer outputs delivers a displacement that can be transformed into rotation, as shown below in Figure 5. Accelerometer weight, noise characteristics and bandwidth determine the achievable angular accuracy and resolution. As part of the simulation, several commercially available accelerometers were tested successfully by modelling their characteristics.

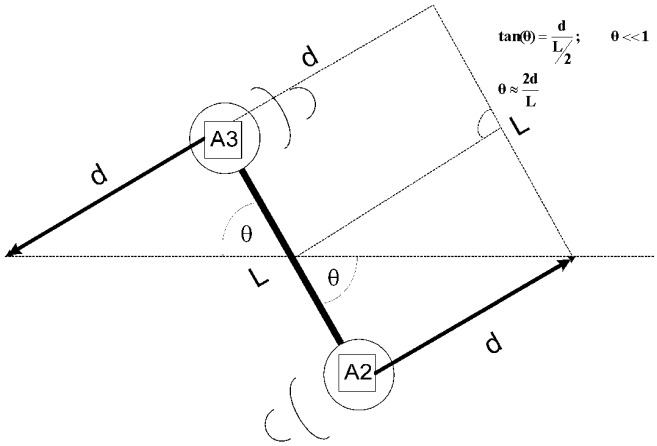


**Figure 5** – Two symmetrically aligned accelerometers measure a rotation rot(t)=1/L*(A2(t) - A3(t))

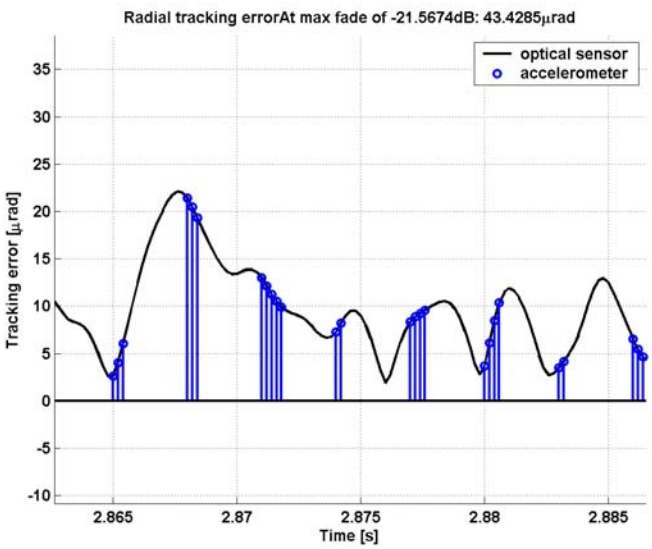


**Figure 6** – Switch to accelerometer feedback during fade

## 4. LINK BUDGET CONSIDERATIONS

Next to mechanical beam steering, the optical antennas had to be modelled, too. The following sections briefly describe the basic equations to be applied for antenna gains and pointing loss at optical frequencies.

*Transmitter Antenna Gain*—For telescopes with Gaussian-beam illumination and a central obscuration $\gamma_{Tx}$, where the obscuration ratio $\gamma_{Tx}$ is defined as ratio of central obscuration diameter to main (Tx) aperture diameter, the on-axis farfield transmitting antenna gain yields [RD 9]:

$$G_{Tx} = \left(\frac{\pi \cdot D_{Tx}}{\lambda}\right)^2 \cdot \frac{2}{\alpha_{Tx}} \cdot \left[e^{-\alpha^2_{Tx}} - e^{-\alpha^2_{Tx}\,\gamma^2_{Tx}}\right]^2, \qquad (1)$$

$$\alpha_{Tx,\,\gamma_{Tx}\le 0.4} = 1.12 - 1.30 \cdot \gamma^2{}_{Tx} - 2.12 \cdot \gamma^4{}_{Tx}$$

The beam truncation ratio is expressed by $\alpha_{TX}$. For an antenna of 15 cm diameter, 10% obscuration and 1064 nm wavelength, GTx = 112 dB.

*Space Loss*—The space loss depends on range and wavelength and is computed by the following equation:

$$SL = \left(\frac{\lambda}{4\pi R_0}\right)^2 \quad R_0 = \text{link distance} \qquad (2)$$

*Receiving Antenna Gain—The* receiving antenna gain is defined as the gain of an ideal receiving aperture with an area equal to the unobscured part of the telescope, taking into account the obscuration $\gamma_{Rx}$ where the obscuration ratio $\gamma_{Rx}$ is defined as ratio of central obscuration diameter to main (Rx) aperture diameter. The effective area is $\pi * D_{Rx}/4 * (1-\gamma^2_{Rx})$ [RD 10].

$$G_{Rx} = \left(\frac{\pi \cdot D_{Rx}}{\lambda}\right)^2 \cdot \left(1 - \gamma^2{}_{Rx}\right) \qquad (3)$$

*BSU Loss Budget*—An additional non-space loss factor is superimposed to the received optical power in the optical link budget, in addition to space loss and optical antenna gains: It comprises contributions of both, the receive- and transmit optical path inside the optical head. and has been taken from the ISLFE terminal budget description [RD 5]. This terminal has been designed for geostationary ISL, using a 135 mm aperture diameter (both, for Tx and Rx) and its overall design parameters stay close to the ones required for the investigated BSU. Based on that reference, the total non-space loss is estimated to -10.7 dB.

## 5. POINTING, ACQUISITION, TRACKING

*Pointing*—Pointing losses occur due to bias pointing effects and due to random pointing jitter about the bias value. In a first approximation, when neglecting point ahead errors, pointing errors are directly related to tracking errors. Additional pointing bias errors occur due to potential optical paths misalignment between Tx and Rx/Tracking.

The composition of random pointing jitter requires special attention because of the two-dimensional nature of the phenomenon: two statistically independent jitter contributions per (orthogonal) pointing axis have to be combined to one single radial pointing jitter value. The overall radial pointing error $\theta_e$ consists of a bias pointing error $\eta$ ($\eta = \sqrt{\eta_x^2 + \eta_y^2}$) and a dynamic pointing error $\theta_e(t) = \sqrt{\theta_x^2(t) + \theta_y^2(t)}$ with an independent Gaussian random process for both, $\theta_x(t)$ and $\theta_y(t)$, where $\sigma_x^2 = \sigma_y^2 = \sigma^2$.

The probability density of the resulting radial pointing error $\theta_e$ can be expressed as the Rice density [RD 7]:

$$p(\theta_e) = \frac{\theta_e}{\sigma^2} \cdot \exp\left[-\frac{1}{\sigma^2} \cdot \left(\theta^2{}_e + \eta^2\right)\right] \cdot I_0\left(\frac{\theta_e \cdot \eta}{\sigma^2}\right) \qquad (4)$$

## 6. CONCLUSIONS

Following the simulation results, a feasibility statement could be derived that allows us to design an optical beam steering accuracy in stratospheric crosslinks within ±70µrad, using a Tx divergence angle of ±190µrad. The two-axis mechanical disturbance profile was modelled based on measurement data from a Zeppelin airship, assuming a worst case of 16 mg rms per axis. Optical channel characteristics in stratosphere were modelled based on parameters from [RD 2], obtaining fade durations of up to several tens of milliseconds and fade depth statistics similar to those shown in Table 1, with maximum attenuation of 50dB.

The outcome of the system simulation showed that state-of-the-art technology is sufficient to provide a robust beam steering unit for use in stratospheric optical crosslinks between high-altitude platforms (HAPs). In contrast to satellite-to-ground links, both optical terminals were located in turbulent medium. The aim of the simulation was to investigate on fade-tolerant beam acquisition and tracking methods, taking into account both, platform vibration, attitude drift and statistical attentuation characteristics of the stratospheric channel. The effect of accelerometer sensors was investigated closer. Latter were used to generate tracking sensor feedback signals during absence of optical feedback from the counter terminal.

## ACKNOWLEDGEMENTS

The present study is partly being funded by BBW in Bern under EU contract number 506745. The authors would like to gratefully acknowledge the contributions on vibration characteristics of airships from Zeppelin Luftschifftechnik GmbH, Friedrichshafen. In addition, we express our gratitude to Dr. U. Somaini and Mr. U Wieland at Contraves Space AG for their continued support in the execution of this work.

## ACRONYMS AND ABBREVIATIONS

| | |
|---|---|
| BSU | Beam Steering Unit |
| DTx | Transmitter effective antenna diameter |
| DRx | Receiver effective antenna diameter |
| ESA | European Space Agency |
| FoV | Field of View |
| HAP | High Altitude Platform |
| ISLFE | Inter Satellite Front End |
| OISL | Optical Inter Satellite Link |
| PAT | Pointing, Acquisition and Tracking |
| Rx | Receive |
| SROIL | Short Range Optical Intersatellite Link |
| Tx | Transmit |

## REFERENCES

[1] "The High Resolution Doppler Imager", University of Michigan, http://hrdi.engin.umich.edu/index.html

[2] "Upper Atmosphere Research Satellite (UARS) Project" Science Office Page, http://umpgal.gsfc.nasa.gov/www_root/homepage/uars-science.html

[3] Karp, S. et. al. "Optical Channels", Plenum Publishing Corporation, 1988, section 1.4.

[4] Radio Corporation of America (RCA): "Electro Optics Handbook, a compendium of useful information and technical data", 1968, pp. 7-8 and 7-11

[5] Baister, G.C. et. al., "The ISLFE Terminal Development Project – Results from The Engineering Breadboard Phase," *20th AIAA International Communication Satellite Systems Conference,* 12th - 15th May 2002

[6] Dreischer, T. et. al. Operating in sub-arc seconds: High Precision Laser Terminals for Intersatellite Communications, *SPIE Conference on Optomechatronic Systems III, Vol. 4902,* 12-14 November 2002

[7] V.A. Vilnrotter "The Effects of Pointing Errors on the Performance of Optical Communication Systems", *TDA Progress Report 42-63*, Mar-Apr 1981

[8] Shinak Lee and Gerardo G. Ortiz, "Atmosphere Tolerant Acquisition, Tracking and Pointing Subsystem", Free-Space Laser Communication Technologies XV, G. Stephen Mecherle, Proceedings of SPIE Vol. 4975, 2003

[9] Klein, B.J., Degnan, J.J. "Optical Antenna Gain, 1: Transmitting Antennas", *Applied Optics, 13*, 9, Sep 1974

[10] Klein, B.J., Degnan, J.J. "Transmitter and Receiver Antenna Gain Analysis for Laser Radar and Communication Systems", *Goddard Space Flight Center, Preprint X-524-73-185*, June 1973

[11] Vernin, J., Munoz-Tunon, C. "Optical Seeing at La Palma Observatory, I. General Guidelines and preliminary results(...)", *Astron. Astrophysics*, 257, 811-816 (1992)